IEEE Photonics Journal
An IEEE Photonics Society Publication

Ultracompact Silicon Waveguide Bends Designed Using a Particle Swarm Optimization Algorithm

Volume 13, Number 1, February 2021

Po-Han Fu
Chen-Yu Chao
Ding-Wei Huang

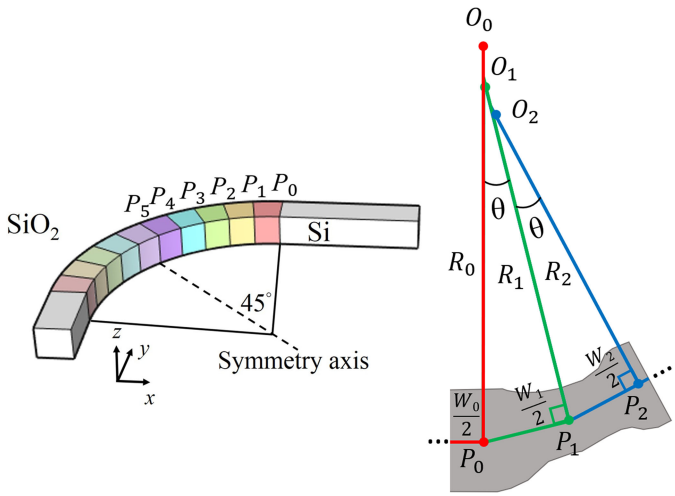

DOI: 10.1109/JPHOT.2020.3043828

Ultracompact Silicon Waveguide Bends Designed Using a Particle Swarm Optimization Algorithm

Po-Han Fu,[1] **Chen-Yu Chao**,[1] **and Ding-Wei Huang**[1,2]

[1]Graduate Institute of Photonics and Optoelectronics, National Taiwan University, Taipei 10617, Taiwan
[2]Department of Electrical Engineering, National Taiwan University, Taipei 10617, Taiwan

DOI:10.1109/JPHOT.2020.3043828

Manuscript received October 20, 2020; revised November 24, 2020; accepted December 7, 2020. Date of publication December 10, 2020; date of current version January 12, 2021. This work was supported by the Ministry of Science and Technology, Taiwan, R.O.C. under Grants MOST106-2221-E-002-140, MOST107-2218-E-992-304, MOST108-2218-E-992-302, MOST109-2221-E-002-185, and MOST109-2224-E-992-001. Corresponding author: Ding-Wei Huang (e-mail: dwhuang@ntu.edu.tw).

Abstract: In this study, the trajectory of a 90° bend is divided into two symmetric halves that are mirror images of each other as referenced to the symmetry axis at 45°, and each half is segmented into small curved sections. The bending radius and waveguide width for every section are parameters to be determined using a particle swarm optimization algorithm. The optimization is performed to maximize the transmission of the waveguide bends, which is calculated by using the three-dimensional finite-difference time-domain technique. The results indicate that the total bending loss of the optimized 90° bends with radii of 2, 3, 4, and 5 μm are 0.0106, 0.0051, 0.0025, and 0.0023 dB, respectively, at the wavelength $\lambda = 1550$ nm. In addition, the optimal devices are fabrication tolerant, with fabrication errors in width and height within 10 nm, and less wavelength-dependent compared with circular bends.

Index Terms: Bends, optical loss, particle swarm optimization, radius of curvature, silicon photonics, waveguides.

1. Introduction

optical waveguides are fundamental elements that connect a wide variety of devices in photonic integrated circuits (PICs) that are used in optical computing, communication, sensing, and so on. For the material system, the silicon-on-insulator (SOI) platform is probably the most promising candidate because an SOI-based PIC can be manufactured using the well-developed complementary metal-oxide-semiconductor (CMOS) technology, which is widely used in integrated circuit manufacturing [1]–[4]. In addition, the large index difference between the silicon waveguide core and the silica cladding allows for tight light confinement within the range of hundreds of nanometers as well as a small bending radius down to a few microns with low bending loss on the order of 0.01 dB over the communication band [5]. Despite the fact that the performance of a single conventional 90° circular waveguide bend is satisfactory, the total bending loss can be significantly accumulated, especially for a large-scale PIC that contains hundreds of waveguide bends. Therefore, further improvement in the performance of waveguide bends to reduce the insertion loss and footprint is highly desired in a PIC.

The total bending loss of a waveguide bend is caused by material absorption, scattering loss due to sidewall roughness, radiation loss, and mode mismatch loss. Among them, material absorption is inherently determined by the material itself and scattering loss due to sidewall roughness is determined by the manufacturing process condition and waveguide width as it influences the mode confinement inside the waveguide and the amount of light interacts with the roughness. Therefore, the reduction of radiation loss and mode mismatch loss are the main ideas for device optimization in this study.

A wide variety of approaches have been developed to reduce the total bending loss of a waveguide bend. For example, mode mismatch loss at the interfaces (the straight-to-bend joints) can be reduced by using taper structures [6] or offsetting the position of straight waveguides such that the positions of mode profiles with maximum power distribution of the straight and bent waveguides are aligned [7]–[9]. In [10], compared with the circular waveguide bend, the authors show that the optimal waveguide bend has larger radius of curvature at the two ends for a better mode matching with straight waveguides. In addition, approaches based on bend trajectory design such as Bezier bend [11], Euler bend for multi-mode waveguides[12], hybrid bend (Euler-circular) [13], adiabatic bend [14], [15], and the bend trajectories of customized functions [16] for designing low-loss waveguide bends on the silicon photonic platform can effectively reduce the total bending loss with the effective bending radius R_{eff} in excess of 3 μm compared with the circular bend with a constant radius of curvature. R_{eff} is defined as follows that the start and end points of the 90° waveguide bend are (0,0) and (R_{eff}, R_{eff}), respectively. The gradual change in curvature helps to avoid the strong mode mismatch loss commonly encountered in a circular bend due to the abrupt change in curvature at the interfaces. However, for a single-mode 220-nm-thick SOI waveguide, as R_{eff} decreases down to 2 μm, the trajectory design techniques proposed in published literature fail to reduce the total bending loss because the radius of curvature at the middle part of the trajectory is considerably smaller than 2 μm, which may lead to severe radiation loss [13]. The design using clothoid curves with angles exceeding 90 degree can be an alternative approach to deal with ultrasmall bending radius ($R_{\mathrm{eff}} = 1.6$ μm) [17]. However, the design methodology is not applicable to a commonly used 90° bend and the light propagation path is obviously detoured, which may increase the device footprint. By using inverse design method, the bending loss can be reduced efficiently compared with circular bends for a multimode waveguide with width exceeding 1 μm for R_{eff} less than 2 μm while the bending loss can be as high as 1 dB/Turn [18].

In this study, we propose a design method for low-loss 90° waveguide bends with ultrasmall bending radii. Not only the trajectory is taken into account, but the waveguide width is also considered so as to provide an additional degree of freedom to optimize the waveguide bend geometry using the particle swarm optimization (PSO) algorithm [19]. The design concept is found to be effective to reduce the total bending loss of waveguide bends with bending radii down to 2 μm.

2. Relationship Between Insertion Loss, Bending Radius, and Waveguide Width

While using the PSO algorithm for optimization, the waveguide widths and the bending radii are taken as parameters for the geometrical design. Before performing the optimization, reasonable lower and upper bounds for all parameters must be determined. The radiation loss in dB/cm as a function of waveguide width for a conventional circular bend with a bending radius R of 1–5 μm is required to determine the range of waveguide widths. However, the total bending loss of a 90° bend consists of the mode mismatch loss part and the radiation loss part, and there is no straightforward way to calculate the radiation loss part using a single simulation. In this study, the radiation loss is calculated by subtracting the total bending loss of a 90° waveguide bend from that of a 180° waveguide bend because the mode mismatch loss part at the interfaces of the straight and bent waveguides is canceled if the waveguide bend supports only the fundamental mode and the mode profile does not change as it propagates within the waveguide bend (i.e.,no change for the curvature

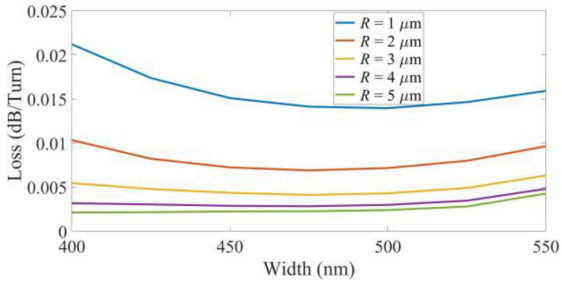

Fig. 1. Radiation loss as a function of waveguide width for R of 1–5 μm.

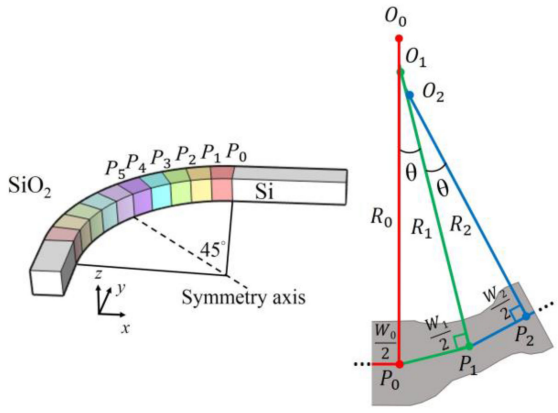

Fig. 2. Schematic for the design method of a waveguide bend.

or waveguide width) [16]. The total bending loss calculations for the fundamental TE mode are performed using the three-dimensional finite-difference time-domain (3-D FDTD) technique and the derived radiation loss is shown in Fig. 1. The mesh grid size $\Delta x \times \Delta y \times \Delta z = 10$ nm $\times$ 10 nm $\times$ 10 nm, which is fine enough to show the accurate result and the refractive indices of silicon and silica are given in [20]. If R is below 3 μm, the curve opens upward and the waveguide width for the minimum radiation loss becomes wider as R decreases. When R exceeds 3 μm, the radiation loss becomes less dependent on the waveguide width. In this study, the range of R_{eff} is 2–5 μm and the range for the waveguide width is determined to be 400–700 nm for the following optimization process. Moreover, Fig. 1 indicates that it is possible to further reduce the radiation loss of a 90° waveguide bend by varying both the trajectory and the waveguide width compared with the one with trajectory design only. A similar concept has been proposed and applied for the optimal design of a 180° waveguide bend [21]. From the literature, it is known that the total bending loss consists of not only radiation loss and mode mismatch loss at the straight-to-bend joints but also mode evolution loss due to the variations of bending radius and width as light propagates through the waveguide bend. The mode evolution loss can be the dominant factor when R_{eff} is small or the bending radius and width vary drastically along the light path. However, there is no straightforward way to separate the mode evolution loss from the radiation loss, and it is not easy to find an analytic function to design the geometry of a 90° waveguide bend. In this case, we define a set of parameters to be optimized that is sufficient to describe the geometry, and the target is to minimize the total bending loss. The optimized solution is eventually carried out by the PSO algorithm.

In this study, the input silicon channel waveguide is chosen to be a commonly used device with dimensions 450 nm $\times$ 220 nm. The 90° waveguide bend is segmented into small curved sections and each curved section has its corresponding radius and width, as shown in Fig. 2. To reduce the complexity during the optimization process, the 45° angle is chosen as the symmetry axis, and each 45° half is divided into five major curved sections with equal spacing of 9°. The joints between these

TABLE 1
Exact Values of G and w_0 for the Optimal Design

Position	Radius (μm) / Width (nm)	R_{eff} 2 μm	R_{eff} 3 μm	R_{eff} 4 μm	R_{eff} 5 μm
P_0	R_0	3.336	4.413	7.371	6.515
	W_0	450	450	450	450
P_1	R_1	3.169	4.428	4.721	5.707
	W_1	479	480	557	506
P_2	R_2	2.170	1.779	4.139	6.254
	W_2	514	523	582	518
P_3	R_3	1.714	3.725	3.577	3.453
	W_3	573	546	585	529
P_4	R_4	1.356	2.368	2.851	4.261
	W_4	636	621	600	540
P_5	R_5	1.111	2.138	3.156	4.899
	W_5	650	650	607	544
Bending Loss (dB/turn)		0.0106	0.0051	0.0025	0.0023

major sections are denoted as P_0, P_1, P_2, P_3, P_4, and P_5. The local bending radii and waveguide widths of the starting point of the n-th major curved section are R_n and W_n, respectively. Each major curved sections can be further refined into minor curved sections with their corresponding bending radii and waveguide widths defined as the interpolations of the bending radii and waveguide widths at its starting and ending joints. The bending radius is calculated from the center of the waveguide to the center of each local curved section (O_0, O_1, O_2, ...). Ideally, the trajectory for light propagation should be smooth to avoid undesired scattering loss, so the bending radius of each minor curved section along the trajectory of the n-th major curved section is determined by linear interpolation (1) while the waveguide width is determined by a smoother cosine-like interpolation (2). The cosine-like interpolation for waveguide width was chosen to keep a continuous mode propagation direction at the interfaces between adjacent major sections.

$$R_{n\to n+1}(t) = R_n + (R_{n+1} - R_n)\times\frac{t}{9}, \tag{1}$$

$$W_{n\to n+1}(t) = W_n + (W_{n+1} - W_n) \times \frac{1}{2} \times \left(1 - \cos\left(\frac{\pi t}{9}\right)\right) \tag{2}$$

where n = 0, 1, 2, 3, 4, and t is the angle (in unit of degree) as referenced to the start point of the n-th major section that $0 \le t \le 9$.

3. Results and Discussion

The goal for the optimization is to minimize the bending loss (to maximize the transmission for the fundamental TE mode). The PSO starts with a set of N possible solutions (particles) with their parameters (i.e., R_n and W_n) randomly generated within the upper and lower bounds that 450 nm $\le W_n \le$ 700 nm and $R_n \ge 1$ μm. The performance of each particle is calculated using a 3-D FDTD simulation provided by a commercial software (Lumerical) that the fundamental TE mode is excited at the input port and the transmission of the fundamental TE mode is calculated at the output port upon finishing the simulation. The set of possible solutions evolves toward a better one over the iterations in a way that the parameters of every particle are updated by the best known parameters of the particle and the entire swarm. The evolution is terminated when the convergence condition is satisfied.

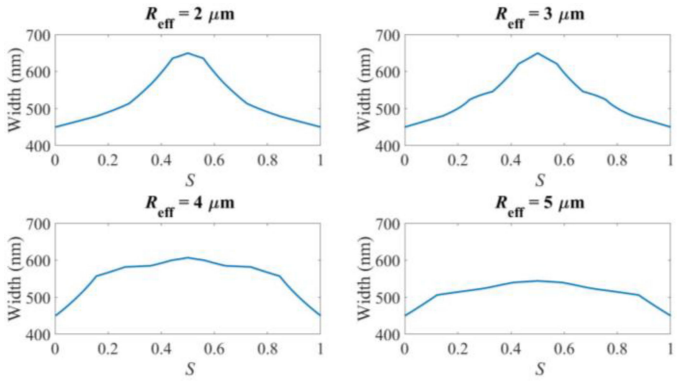

Fig. 3. Width versus length of the normalized light path S of the optimal design.

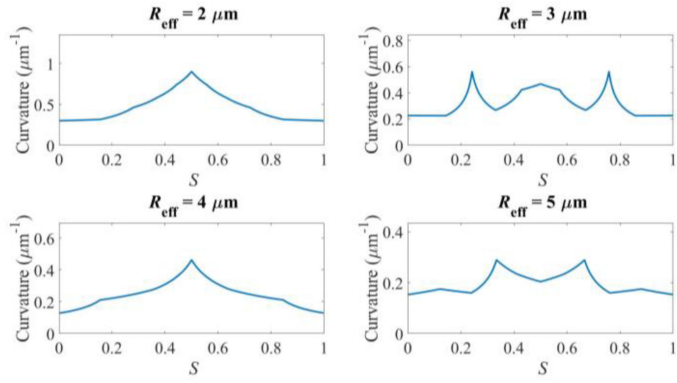

Fig. 4. Curvature (R^{-1}) versus length of the normalized light path S of the optimal design.

The optimal design parameters for $R_{\text{eff}} = 2$, 3, 4, and 5 μm are listed in Table 1. For the optimal design, the waveguide width gradually increases from the starting point of the waveguide bend for all R_{eff} while the variation of curvature shows no consistency which can be attributed to multimode interference effects … The width and the curvature (R^{-1}) versus the normalized light path S (the total light path is normalized to 1) of the optimal design for $R_{\text{eff}} = 2$, 3, 4, and 5 μm are shown in Fig. 3 and Fig. 4, respectively. Note that the curvatures are not zero at the junctions between the 90° waveguide bend and the straight waveguides for the optimal design, which may induce the mode mismatch loss. However, the overall bending loss can be reduced and the reduced radiation loss can compensate for the mode mismatch loss because an additional degree of freedom is provided for optimization. Moreover, large W may result in a reduced radiation loss for large curvature while higher modes may be excited. As the waveguide structure varies, the higher modes can be coupled back to the fundamental mode as the light propagates and result in a reduced overall bending loss. The normalized power distributions (in log scale) for $\lambda = 1550$ nm at half the height of the silicon waveguide core for the circular and optimal waveguide bends calculated using 3-D FDTD simulation are shown in Fig. 5. For $R_{\text{eff}} = 3$, 4, and 5 μm, the design using Euler curve bends and optimal solutions effectively reduce the mode mismatch loss caused by mismatch at the interfaces of the straight waveguide and waveguide bend compared with circular bends with constant radii. Note that for R_{eff} as small as 2 μm for a 220-nm-thick SOI waveguide, by designing not only the waveguide trajectory but also the width, the total bending loss of the optimal design can be further reduced compared with circular waveguide bends where other waveguide bend designs reported to date failed to reduce the total bending loss [13].

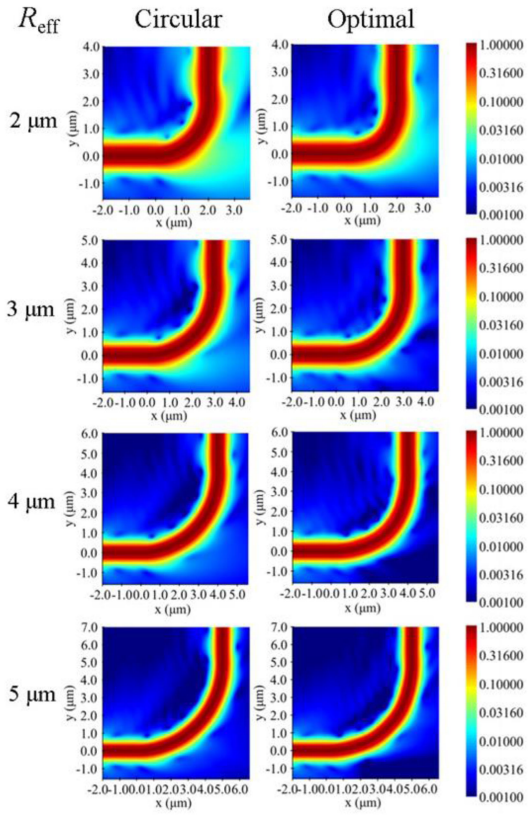

Fig. 5. Normalized power distributions for $\lambda = 1550$ nm at $z = 0.11$ μm in log scale for circular and optimal waveguide bends calculated using 3-D FDTD simulation.

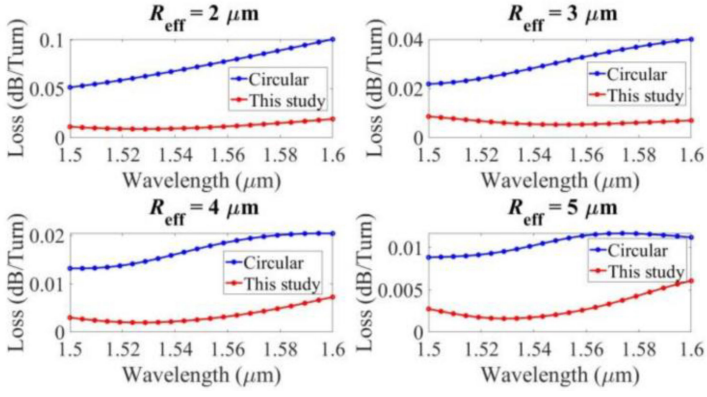

Fig. 6. Spectral response of the bending loss of circular and optimal waveguide bends for $\lambda = 1500$–1600 nm.

The spectral response of the bending loss of the circular and the optimal waveguide bends for $\lambda = 1500$–1600 nm for $R_{\text{eff}} = 2$, 3, 4, and 5 μm is shown in Fig. 6. Over the 100-nm spectral range, the bending loss and the wavelength dependence of the optimal design are lower than those of the circular bends for all values of R_{eff}. Table 2 shows the comparison of previously demonstrated 90° waveguide bends of $R_{\text{eff}} = 2$, 3, 4, and 5 μm on an SOI platform with regard to the total bending loss based on simulations. Note that the optical loss can be larger when they are fabricated

TABLE 2
Comparison of 90° Waveguide Bends with Published Values From the Literature (Numerical Result)

Reference	Width (nm)	Bending Loss (dB/turn)			
		R_{eff} 5 μm	R_{eff} 4 μm	R_{eff} 3 μm	R_{eff} 2 μm
Circular [16]	400	0.0108	0.0200	0.039	0.106
Bezier [16]	400	0.0025	0.0058	0.037	0.224
Euler [16]	400	0.0031	0.0077	0.033	0.241
Hybrid [16]	400	0.0021	0.0041	0.021	0.124
Optimal [16]	400	0.0016	0.0033	0.012	0.116
Circular	450	0.0115	0.0174	0.031	0.074
This Work	450	0.0023	0.0025	0.005	0.011

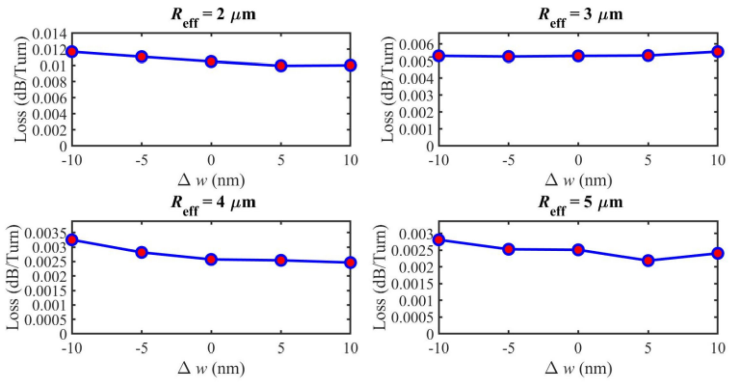

Fig. 7. Total bending loss of 90° bends at $\lambda = 1550$ nm caused by fabrication error in width.

since the scattering loss due to waveguide surface roughness and material absorption loss are not taken into consideration. As shown, the presented optimal design in this study exhibits significant performance improvement for $R_{\text{eff}} = 2$–$5\ \mu$m compared with circular bends. For waveguide bends with larger radius (e.g., $R_{\text{eff}} = 5\ \mu$m), owing to the low radiation loss and slight variation of the curvature, the 90° waveguide bend can be assumed to be adiabatic so that the dominant factor for total bending loss is the mode mismatch loss at the straight-to-bend joints. In this manner, the design strategy to ensure zero curvature at the straight-to-bend joints can be effective in reducing the total bending loss. However, such an approach is no longer effective for $R_{\text{eff}} = 2\ \mu$m because the radiation loss can be higher for the 90° waveguide bend. Moreover, due to the abrupt change of the curvature within a short distance, the 90° waveguide bend cannot be viewed as an adiabatic device. It should be noted that the optimal design for this work has significant performance improvement, especially for $R_{\text{eff}} = 2\ \mu$m. It shows great potential in reducing the footprint for the development of PICs.

4. Fabrication Tolerance Analysis

The variation of total bending loss of 90° waveguide bends at $\lambda = 1550$ nm for $R_{\text{eff}} = 2$, 3, 4, and 5 μm caused by fabrication errors in width and height are shown in Fig. 7 and Fig. 8, respectively. It is assumed that the central positions of the silicon waveguides are fixed, and Δw and Δh are the fabrication errors for waveguide width and height, respectively, which deviate from the ideal design. For Δw and Δh, five points are taken into account with a uniform spacing of 5 nm in the range from -10 to 10 nm. The maximum total bending loss in dB/turn for $R_{\text{eff}} = 2$, 3, 4, and 5 μm are 0.0117, 0.0055, 0.0032, and 0.0028 dB, respectively, for the variation of Δw, and 0.0136, 0.0055,

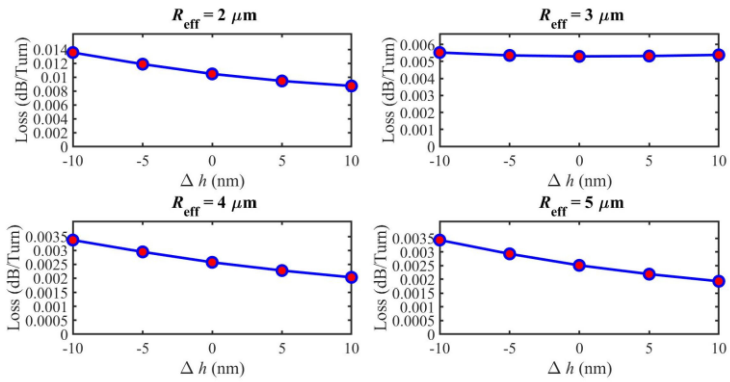

Fig. 8. Total bending loss of 90° bends at $\lambda = 1550$ nm caused by fabrication error in height.

0.0034, and 0.0034 dB, respectively, for the variation of Δh. The result indicates that the device performance is slightly more sensitive to Δh compared with Δw, and is still robust even for Δw and Δh up to $\pm$10 nm.

5. Conclusion

For a 90° waveguide bend with constant width, results from the literature indicate that the total bending loss cannot be reduced for $R_{\text{eff}} = 2$ μm by designing the bend trajectory because the bending radius can be very small near the middle part, along with severe radiation loss for 220-nm-thick SOI waveguides. In this study, we propose a design method for low-loss 90° waveguide bends with ultrasmall bending radii for 220-nm-thick SOI waveguides. Both trajectory and waveguide width are considered. The 90° waveguide bend is segmented into small curved sections and the bending radius and waveguide width of every section is optimized by the PSO algorithm. The result indicates that the bending loss can still be reduced for a bending radius down to 2 μm, along with robust fabrication tolerance. The authors believe that the design concept in this study is effective in reducing the footprint for the development of PICs.

References

[1] B. Jalali and S. Fathpour, "Silicon photonics," *J. Lightw. Technol.*, vol. 24, no. 12, pp. 4600–4615, Dec. 2006.
[2] W. Bogaerts and L. Chrostowski, "Silicon photonics circuit design: Methods, tools and challenges," *Laser Photon. Rev.*, vol. 12, Apr. 2018, Art. no. 1700237.
[3] J. S. Orcutt and R. J. Ram, "Photonic device layout within the foundry CMOS design environment," *IEEE Photon. Technol. Lett.*, vol. 22, no. 8, pp. 544–546, Apr. 2010.
[4] R. Soref, "The past, present, and future of silicon photonics," *IEEE J. Sel. Topics Quantum Electron.*, vol. 12, no. 6, pp. 1678–1687, Nov./Dec. 2006.
[5] Y. A. Vlasov and S. J. McNab, "Losses in single-mode silicon-on-insulator strip waveguides and bends," *Opt. Exp.*, vol. 12, pp. 1622–1631, Apr. 2004.
[6] H. Shen, L. Fan, J. Wang, J. C. Wirth, and M. Qi, "A taper to reduce the straight-to-bend transition loss in compact silicon waveguides," *IEEE Photon. Technol. Lett.*, vol. 22, no. 15, pp. 1174–1176, Aug. 2010.
[7] M. K. Smit, E. C. M. Pennings, and H. Blok, "A normalized approach to the design of low-loss optical waveguide bends," *J. Lightw. Technol.*, vol. 11, no. 11, pp. 1737–1742, Nov. 1993.
[8] D. Dai and Y. Shi, "Deeply etched SiO_2 ridge waveguide for sharp bends," *J. Lightw. Technol.*, vol. 24, no. 12, pp. 5019–5024, Dec. 2006.
[9] S. Chulhun and J. C. Chen, "Low transition losses in bent rib waveguides," *J. Lightw. Technol.*, vol. 14, no. 10, pp. 2255–2259, Oct. 1996.
[10] Z. Hu and Y. Y. Lu, "Computing optimal waveguide bends with constant width," *J. Lightw. Technol.*, vol. 25, no. 10, pp. 3161–3167, Oct. 2007.
[11] H. P. Bazargani, J. Flueckiger, L. Chrostowski, and J. Azaña, "Microring resonator design with improved quality factors using quarter bezier curves," in *Proc. Conf. Lasers Electro-Opt.*, Aug. 2015, pp. 1–2.
[12] M. Cherchi, S. Ylinen, M. Harjanne, M. Kapulainen, and T. Aalto, "Dramatic size reduction of waveguide bends on a micron-scale silicon photonic platform," *Opt. Exp.*, vol. 21, pp. 17814–17823, Jul. 2013.

[13] T. Fujisawa, S. Makino, T. Sato, and K. Saitoh, "Low-loss, compact, and fabrication-tolerant Si-wire 90° waveguide bend using clothoid and normal curves for large scale photonic integrated circuits," *Opt. Exp.*, vol. 25, pp. 9150–9159, Apr. 2017.
[14] W. Bogaerts and S. K. Selvaraja, "Compact single-mode silicon hybrid rib/strip waveguide with adiabatic bends," *IEEE Photon. J.*, vol. 3, no. 3, Jun. 2011.
[15] T. Chen, H. Lee, J. Li, and K. J. Vahala, "A general design algorithm for low optical loss adiabatic connections in waveguides," *Opt. Exp.*, vol. 20, pp. 22819–22829, Sep. 2012.
[16] M. Bahadori, M. Nikdast, Q. Cheng, and K. Bergman, "Universal design of waveguide bends in silicon-on-insulator photonics platform," *J. Lightw. Technol.*, vol. 37, no. 13, pp. 3044–3054, Jul. 2019.
[17] M. Nakai, T. Nomura, S. Chung, and H. Hashemi, "Geometric loss reduction in tight bent waveguides for silicon photonics," in *Proc. Conf. Lasers Electro-Opt.*, San Jose, CA, 2018, pp. 1–2.
[18] Y. Liu *et al.*, "Very sharp adiabatic bends based on an inverse design," *Opt. Lett.*, vol. 43, pp. 2482–2485, May. 2018.
[19] J. Kennedy and R. Eberhart, "Particle swarm optimization," in *Proc. Int. Conf. Neural Netw.*, vol. 4, pp. 1942–1948, 1995.
[20] E.D. Palik, *Handbook of Optical Constants of Solids.*, 1st ed., Academic Press, 1985.
[21] C. Koos, C. G. Poulton, L. Zimmermann, L. Jacome, J. Leuthold, and W. Freude, "Ideal bend contour trajectories for single-mode operation of low-loss overmoded waveguides," *IEEE Photon. Technol. Lett.*, vol. 19, no. 11, pp. 819–821, Jun. 2007.